Selection in two-sex structured populations

de Vries, C.

Publication date
2019
Document Version
Other version
License
Other

[Link to publication](#)

Citation for published version (APA):
de Vries, C. (2019). *Selection in two-sex structured populations*. [Thesis, fully internal, Universiteit van Amsterdam].

4

Density-dependent selection in one-sex stage-structured populations

Charlotte de Vries, Robert A. Desharnais, Hal Caswell

Abstract

The study of eco-evolutionary dynamics is based on the idea that ecological and evolutionary processes may operate on the same, or very similar, time scales, and that interactions of ecological and evolutionary processes may have important consequences. Here we develop a model that combines Mendelian population genetics with nonlinear demography to create a truly eco-evolutionary model. We use the vec-permutation matrix approach, classifying individuals by stage and genotype. The demographic component is female dominant and density-dependent. The genetic component includes random mating by stage and genotype, and arbitrary effects of genotype on the demographic phenotype. Mutation is neglected. The result is a nonlinear matrix population model that projects stage × genotype dynamics. We show that the results can include bifurcations of population dynamics driven by the response to selection. We present analytical criteria that determine whether one allele excludes the other or if they persist in a protected polymorphism. The analysis is based on local stability analysis of the homozygous boundary equilibria.

As an example, we use a density-dependent stage-classified model of the flour beetle *Tribolium castaneum*. Our model permits arbitrary life-cycle complexity and nonlinearity. *Tribolium* has developed resistance to the pesticide malathion due to a dominant allele at a single autosomal locus. Using parameters reported from laboratory experiments, we show that the model successfully describes the dynamics of both resistant and susceptible homozygotes, and the outcome of a selection experiment containing both alleles. Stability analysis of the boundary equilibria confirms that the resistant allele excludes the susceptible allele, even in the absence of malathion, agreeing with previously reported results.

4.1 Introduction

The demographic processes of birth and death drive changes in gene frequencies and changes in population density and structure. Demography is therefore central to understanding ecology and evolution, and eco-evolutionary analyses always strive to incorporate the fundamental demographic processes of birth, death, and development (e.g., Coulson et al. 2006; Metcalf and Pavard 2007). de Vries and Caswell (2018a) recently introduced an eco-evolutionary framework that combines matrix population models with basic Mendelian genetics. Here we use this framework to explore density-dependent selection.

Density dependence occurs when the per-capita vital rates (rates of birth, mortality, and development) depend on population size or density. Density dependence may be negative or positive (Allee effects). In models that contain demographic structure, "density" is a multivariate concept. Vital rates may depend on the abundance of a particular stage or age class, or on a weighted density that gives distinct weights to different stages rather than the total population density (Caswell et al. 2004) . For example, density-dependent effects due to difficulty in finding mates leads to fertilities that depend on the abundances or densities of reproducing stages. Cannabilism is usually restricted to large individuals eating smaller conspecifics, so density-dependent effects due to cannibalism are size- or stage-specific. We will assume that genotypes can differ in age- or stage-specific rates of development, survival, or fertility anywhere in the life cycle. Thus, we assume that pleiotropic effects are the rule rather than the exception.

Early theoretical work on density-dependent selection (MacArthur 1962; Roughgarden 1971) combined population genetics with unstructured ecological models by writing genotype fitnesses as a function of genotypic densities. MacArthur and Wilson (1967) and Roughgarden (1971) extended the logistic equation to multiple competing genotypes, and showed that selection leads to an increase in population density in a constant environment because only alleles with heterozygote advantage in the carrying capacity can invade, leading to the ideas of r and K selection. Charlesworth (1971) showed this is true for any fitness function that decreases with population densities. Charlesworth (1994) used discrete difference equations to model density-dependent selection in age-structured populations. In this paper, we will incorporate age or stage structure by using matrix population models rather than scalar difference equations.

In this paper we show how to construct a density-dependent Mendelian matrix population model, based on genotype-specific demographic measurements. We show how to use that model to project stage×genotype dynamics, and determine analytical conditions that determine whether alleles will coexist in a genetic poly-

morphism, or if one or another allele will go to fixation. We apply the analysis to a study of pesticide resistance in *Tribolium* beetles, a species that is a pest of stored grain products. We investigate the effect of incomplete dominance on the speed of invasion and on the outcome of invasion using evolutionary stability analysis in Section 4.5.

4.2 Model Construction

Individuals are jointly classified by stage $(1, \ldots, \omega)$, and by genotype $(1, \ldots, g)$. Each genotype is characterized by a survival and transition matrix, and a matrix of fertility rates. Both the transition matrices and the fertility matrices are assumed to be density dependent. In this section, we will consider general density dependence without specifying a functional dependence. In Section 4.3, we apply the general results obtained to a specific model with density-dependent demographic rates.

We make the important assumption of female demographic dominance, i.e. we assume that enough males are always present to fertilize all the females and that the number of offspring produced in a mating is not affected by the stage or genotype (i.e. the i-state) of the male. This assumption can be relaxed by introducing a marriage function, but we do not explore that here. We also assume that males and females have the same survival and transition rates, and that male and female offspring are produced in equal proportions. These two assumptions imply that the male and female genotype×stage population vectors remain equal provided they start equal (de Vries and Caswell 2018b). Therefore we can use the female vector as representative of both the male and the female populations, and we can calculate allele frequencies in the breeding population from the female population vector. These assumptions make it possible to model sexual reproduction in a one-sex model.

For a single locus with 2 alleles, say A and a, we will identify genotypes 1, 2, and 3 as AA, Aa, and aa, respectively. The population state vector is

$$\tilde{\mathbf{n}}(t) = \begin{pmatrix} \mathbf{n}_{AA}(t) \\ \mathbf{n}_{Aa}(t) \\ \mathbf{n}_{aa}(t) \end{pmatrix}. \tag{4.1}$$

where, e.g., $\mathbf{n}_{AA}$ contains the numbers or densities of stages $1, \ldots, s$ for genotype AA.

The matrices, vectors and mathematical operations used in this paper are listed in Table 4.1.

Symbol	Definition	Dimension
a	Number of alleles (2)	
g	Number of genotypes (3)	
ω	Number of stages	
N	Total population size	
N_{b}	Breeding population size	
$\mathbf{c}_i$	Indicator vector for breeding stages in genotype i	$\omega \times 1$
$\tilde{\mathbf{n}}$	Joint stage-genotype vector	$\omega g \times 1$
$\tilde{\mathbf{p}}$	Joint stage-genotype frequency vector	$\omega g \times 1$
$\mathbf{p}_i$	Genotype frequency vector in genotype i	$g \times 1$
$\mathbf{p}'_i$	Genotype frequency vector of offspring of genotype i	$g \times 1$
$\mathbf{q}_i$	Gene frequency vector in genotype i	$a \times 1$
$\mathbf{q}$	Gene frequency vector in gametes	$a \times 1$
$\mathbf{I}_\omega$	Identity matrix	$\omega \times \omega$
$\mathbf{1}_g$	Vector of ones	$g \times 1$
$\mathbf{e}_i$	The ith unit vector, with a 1 in the ith entry and zeros elsewhere.	various
$\mathbf{E}_{ij}$	A matrix with a 1 in the (i,j) position, and zeros elsewhere.	various
$\otimes$	Kronecker product	
vec$\mathbf{X}$	The vec operator, which stacks the columns of an $m \times n$ matrix $\mathbf{X}$ into a $mn \times 1$ vector.	
$\mathbf{U}_i$	Demographic transitions for genotype i	$\omega \times \omega$
$\mathbf{F}_i$	Fertility matrix for genotype i	$\omega \times \omega$
$\mathbf{F}'_i$	Male mating success matrix for genotype i	$\omega \times \omega$
$\mathbf{D}_i$	Genotype transitions for stage i	$g \times g$
$\mathbf{H}_i\left(\tilde{\mathbf{n}}\right)$	Parent-offspring genotype map for stage i	$g \times g$

Table 4.1: Mathematical notation used in this paper. Dimensions of vectors and matrices are given where relevant.

The population vector $\tilde{\mathbf{n}}$ is projected from time t to time $t+1$ by a denisty-dependent matrix $\tilde{\mathbf{A}}\left(\tilde{\mathbf{n}}\right)$, so that

$$
\begin{aligned}
\tilde{\mathbf{n}}(t+1) &= \tilde{\mathbf{A}}\left(\tilde{\mathbf{n}}\right)\tilde{\mathbf{n}}(t), & (4.2) \\
&= \left[\tilde{\mathbf{U}}\left(\tilde{\mathbf{n}}\right) + \tilde{\mathbf{F}}\left(\tilde{\mathbf{n}}\right)\right]\tilde{\mathbf{n}}(t) & (4.3)
\end{aligned}
$$

where $\tilde{\mathbf{U}}$ describes survival and transition rates and $\tilde{\mathbf{F}}$ describes the generation of new individuals by reproduction. The projection matrix $\tilde{\mathbf{A}}$ depends on $\tilde{\mathbf{n}}$ because of genetics (the genotypes of offspring depend on gene frequencies of parents) and because of ecological nonlinearities due to density dependence. The genetic component of the model depends on the normalized population distribution vector,

$\tilde{\mathbf{p}}(t)$, defined as

$$\tilde{\mathbf{p}}(t) = \frac{\tilde{\mathbf{n}}(t)}{\|\tilde{\mathbf{n}}(t)\|}. \tag{4.4}$$

The normalized population distribution vector consists of three genotype-specific population vectors:

$$\tilde{\mathbf{p}}(t) = \begin{pmatrix} \mathbf{p}_{AA}(t) \\ \mathbf{p}_{Aa}(t) \\ \mathbf{p}_{aa}(t) \end{pmatrix}. \tag{4.5}$$

The components of the projection matrix

The projection matrix is constructed from two sets of matrices describing demographic transitions for each genotype, and one set of matrices describing the parent-offspring map for each stage:

$\mathbf{U}_i(\tilde{\mathbf{n}})$ demographic transitions for females of genotype i, $i = 1, \ldots g$ $\omega \times \omega$
$\mathbf{F}_i(\tilde{\mathbf{n}})$ fertility matrix for females of genotype i, $i = 1, \ldots, g$ $\omega \times \omega$
$\mathbf{H}_j(\tilde{\mathbf{n}})$ parent-offspring map for stage j, $j = 1, \ldots, s$ $g \times g$

The matrix $\mathbf{U}_i(\tilde{\mathbf{n}})$ contains the stage-specific (density-dependent) transition and survival rates for females of genotype i. The matrix $\mathbf{F}_i(\tilde{\mathbf{n}})$ contains stage-specific (density-dependent) fertility rates for females of genotype i. The matrices $\mathbf{H}_j(\tilde{\mathbf{n}})$ map the genotype of a mother in stage j to the genotypes of her offspring. The (k, ℓ) entry of $\mathbf{H}_j$ is the probability that the offspring of a genotype ℓ mother, of stage j, has genotype k. We assume that mating is random with respect to stage and hence that the parent-offspring map is the same for all stages, i.e. $\mathbf{H}_j(\tilde{\mathbf{n}}) = \mathbf{H}(\tilde{\mathbf{n}})$ (assortative mating by stage would lead to differences among the $\mathbf{H}_j$). The matrix $\mathbf{H}(\mathbf{n})$ is discussed in the next section. The model also formally contains matrices describing the transitions of individuals among genotype classes for each age or stage (Caswell et al. 2018), but since individuals do not change genotypes these are identity matrices.

Mating: from genotypes of parents to genotypes of offspring[1].

Non-reproductive (e.g., immature) stages play no role in mating, so we define the breeding population by an indicator vector $\mathbf{c}_j$, for $j = 1, \ldots, g$, that shows which stages of genotype j take part in mating. The ith entry of $\mathbf{c}_j$ is 1 if stage i of genotype j reproduces, and 0 otherwise. The size of the breeding population is then

$$N_{\mathrm{b}} \quad = \quad \sum_{i=1}^{g} \left(\mathbf{e}_i^{\mathsf{T}} \otimes \mathbf{c}_i^{\mathsf{T}} \right) \tilde{\mathbf{n}}, \tag{4.6}$$

---

[1]Based on de Vries and Caswell (2018*a*)

where $\mathbf{e}_i$ is a vector $(g \times 1)$ with a 1 in position i and zeros elsewhere, and $\otimes$ indicates the Kronecker product. Breeding stages are allowed to differ among genotypes, in order to study the fate of traits that change reproductive schedules. In the special case where the genotypes do not differ in their reproductive stages, $\mathbf{c}_i = \mathbf{c}$ for all genotypes i and

$$N_{\mathrm{b}} = \left(\mathbf{1}_g^{\mathsf{T}} \otimes \mathbf{c}^{\mathsf{T}}\right) \tilde{\mathbf{n}}, \tag{4.7}$$

where $\mathbf{1}_g^{\mathsf{T}}$ is a vector of ones of dimensions $1 \times g$.

The genotype frequency vector within the breeding population is

$$\mathbf{p}_{\mathrm{b}} = \frac{\mathbf{X}\tilde{\mathbf{n}}}{N_{\mathrm{b}}}. \tag{4.8}$$

where

$$\mathbf{X} = \sum_{i=1}^{g} \left(\mathbf{E}_{ii} \otimes \mathbf{c}_i^{\mathsf{T}}\right) \tag{4.9}$$

with $\mathbf{E}_{ii}$ a matrix of dimension $g \times g$ with a 1 in the (i, i) location and zeros elsewhere. If the breeding vectors are the same for all genotypes, $\mathbf{c}_i = \mathbf{c}$, then

$$\mathbf{X} = \left(\mathbf{I}_g \otimes \mathbf{c}^{\mathsf{T}}\right). \tag{4.10}$$

The genotype frequency vector for genotype i is (trivially) $\mathbf{p}_i = \mathbf{e}_i$.

The gene frequencies in an individual of genotype i, $\mathbf{q}_i$, and the gene frequencies in the breeding population, $\mathbf{q}_{\mathrm{b}}$, are a function of the genotype frequencies, so that

$$\mathbf{q}_i = \mathbf{W}\mathbf{p}_i, \tag{4.11}$$
$$\mathbf{q}_{\mathrm{b}} = \mathbf{W}\mathbf{p}_{\mathrm{b}}, \tag{4.12}$$

where

$$\mathbf{W} = \begin{pmatrix} 1 & 0.5 & 0 \\ 0 & 0.5 & 1 \end{pmatrix}. \tag{4.13}$$

Combining equations (4.8) and (4.12) yields the following expression for the gene frequencies in the breeding population

$$\mathbf{q}_{\mathrm{b}} = \begin{pmatrix} q_A^{\mathrm{b}} \\ q_a^{\mathrm{b}} \end{pmatrix} = \frac{\mathbf{W}\mathbf{X}\tilde{\mathbf{n}}}{N_{\mathrm{b}}}. \tag{4.14}$$

We set mutation rates to zero; see de Vries and Caswell (2018a) for details on how mutation can be included.

The matrix H

When a female randomly picks an allele out of the gamete pool, she will pick allele A with probability q_A^b, and allele a with probability q_a^b. These probabilities therefore determine the distribution of genotypes in her offspring, which is captured in the matrix $\mathbf{H}(\tilde{\mathbf{p}})$,

$$\mathbf{H}(\tilde{\mathbf{p}}) = \begin{pmatrix} q_A^b & \frac{1}{2}q_A^b & 0 \\ q_a^b & \frac{1}{2} & q_A^b \\ 0 & \frac{1}{2}q_a^b & q_a^b \end{pmatrix}. \tag{4.15}$$

The first column of $\mathbf{H}(\tilde{\mathbf{p}})$ contains the genotype distribution of the offspring of an AA mother; she produces an AA offspring with probability q_A^b and an Aa offspring with probability q_a^b. The second and third columns give the genotype distributions for mothers of genotypes Aa and aa. The matrix $\mathbf{H}$ is a homogenous of degree zero function of its argument. Thus we can write it equally as a function of $\tilde{\mathbf{n}}$ or $\tilde{\mathbf{p}}$. For a step by step derivation of $\mathbf{H}$, see section de Vries and Caswell (2018a, Section 2.3 and Appendix A).

The population projection matrix

To project the eco-evolutionary dynamics, the component matrices, $\mathbf{U}_i(\tilde{\mathbf{n}})$ and $\mathbf{F}_i(\tilde{\mathbf{n}})$ must be incorporated into the population projection matrix, $\tilde{\mathbf{A}}(\tilde{\mathbf{n}})$ (e.g., Caswell et al. 2018). To do so, create a set of block-diagonal matrices $\mathbb{U}$, $\mathbb{F}$, and $\mathbb{H}$ that contain the corresponding demographic matrices on the diagonal, i.e.

$$\mathbb{U} = \sum_{i=1}^{g} \mathbf{E}_{ii} \otimes \mathbf{U}_i(\tilde{\mathbf{n}}), \tag{4.16}$$

$$\mathbb{F} = \sum_{i=1}^{g} \mathbf{E}_{ii} \otimes \mathbf{F}_i(\tilde{\mathbf{n}}), \tag{4.17}$$

$$\mathbb{H} = \mathbf{I}_\omega \otimes \mathbf{H}(\tilde{\mathbf{p}}). \tag{4.18}$$

The fertility matrix $\tilde{\mathbf{F}}(\tilde{\mathbf{n}})$ is constructed from the block matrix containing genotype-specific fertility rates and from the parent-to-offspring genotype map,

$$\tilde{\mathbf{F}}(\tilde{\mathbf{n}}) = \mathbf{K}^\mathsf{T}\mathbb{H}(\tilde{\mathbf{p}})\mathbf{K}\mathbb{F}(\tilde{\mathbf{n}}). \tag{4.19}$$

where $\mathbf{K}$ is the vec-permutation matrix (Henderson and Searle 1981), which changes the arrangement of the vector from stages-within-genotypes to genotypes-within-stages. From right to left, the block-diagonal matrix $\mathbb{F}$ first produces offspring, possibly of different birth stages (e.g., seedlings of different sizes) as a function of the genotype of the mother. When they appear, these offspring are associated with the genotype of the mother. The vec-permutation matrix $\mathbf{K}$ rearranges the vector, and then the block-diagonal matrix $\mathbb{H}(\tilde{\mathbf{p}})$ allocates the offspring

to their genotypes, based on the genotype of their mother and the genotype distribution of the rest of the population. Finally, $\mathbf{K}^\mathsf{T}$ returns the vector to its original orientation.

The fertility matrix $\tilde{\mathbf{F}}(\mathbf{n})$ captures the process of Mendelian inheritance. Substituting equation (4.15), (4.17) and (4.18) into equation (4.19) yields

$$\tilde{\mathbf{F}}(\tilde{\mathbf{n}}) = \left(\begin{array}{c|c|c} q_A^{\mathrm{b}}\mathbf{F}_{AA}(\tilde{\mathbf{n}}) & \frac{1}{2}q_A^{\mathrm{b}}\mathbf{F}_{Aa}(\tilde{\mathbf{n}}) & \mathbf{0} \\ \hline q_a^{\mathrm{b}}\mathbf{F}_{AA}(\tilde{\mathbf{n}}) & \frac{1}{2}\mathbf{F}_{Aa}(\tilde{\mathbf{n}}) & q_A^{\mathrm{b}}\mathbf{F}_{aa}(\tilde{\mathbf{n}}) \\ \hline \mathbf{0} & \frac{1}{2}q_a^{\mathrm{b}}\mathbf{F}_{Aa}(\tilde{\mathbf{n}}) & q_a^{\mathrm{b}}\mathbf{F}_{aa}(\tilde{\mathbf{n}}) \end{array} \right). \tag{4.20}$$

The first block column of $\tilde{\mathbf{F}}(\tilde{\mathbf{n}})$ contains the offspring produced by an AA female. The upper left block in the first column, $q_A\mathbf{F}_{AA}(\tilde{\mathbf{n}})$, gives the production of AA offspring by AA females that randomly pick allele A from the gamete pool, which happens with probability q_A. The next block down, $q_a\mathbf{F}_{AA}(\tilde{\mathbf{n}})$, contains the production of of Aa offspring by an AA female picking allele a from the gamete pool. Similarly, the second and third row blocks contain offspring produced by an Aa female and an aa female, respectively.

Since individuals do not change their genotype once they are born, the survival matrix is the block diagonal matrices,

$$\tilde{\mathbf{U}}(\tilde{\mathbf{n}}) = \mathbf{K}^\mathsf{T}\mathbf{I}_{\omega g}\mathbf{K}\mathbb{U} = \mathbb{U}, \tag{4.21}$$

or written in terms of the genotype-specific block matrices,

$$\tilde{\mathbf{U}}(\tilde{\mathbf{n}}) = \left(\begin{array}{c|c|c} \mathbf{U}_{AA}(\tilde{\mathbf{n}}) & \mathbf{0} & \mathbf{0} \\ \hline \mathbf{0} & \mathbf{U}_{Aa}(\tilde{\mathbf{n}}) & \mathbf{0} \\ \hline \mathbf{0} & \mathbf{0} & \mathbf{U}_{aa}(\tilde{\mathbf{n}}) \end{array} \right). \tag{4.22}$$

We project the stage×genotype dynamics with $\tilde{\mathbf{U}}(\tilde{\mathbf{n}})$ in equation (4.22) and $\tilde{\mathbf{F}}(\tilde{\mathbf{n}})$ in equation (4.20), using equation (4.3).

4.3 Stage ×genotype dynamics of *Tribolium*

Flour beetles of the genus *Tribolium* have been used extensively to study population dynamics and population genetics, see Costantino et al. (2005) for a review. *Tribolium* is an economically important pest of flour and stored grain products. A nonlinear matrix population model for *Tribolium* was developed by Cushing and collaborators, see for example Cushing et al. (2002). The *Tribolium* model contains three stages: larvae (L), pupae (P), and adults (D). It is nonlinear because, in addition to feeding on flour, *Tribolium* adults cannibalize eggs and larvae; larvae in turn cannibalize eggs. These nonlinearities lead to a plethora of

interesting bifurcations, attractors, and transient and asymptotic dynamics, which have been studied extensively (Costantino et al. 1995, 1997, 2005; Henson et al. 2002; Cushing et al. 2002; Edmunds et al. 2003).

We use the *Tribolium* model as the basis for a genetic model by including one-locus, two allele (A and a) Mendelian genetics.

We define effective adult densities D^* and $D^\dagger$, and an effective larval density $L^\dagger$, as linear combinations of the genotype densities

$$
\begin{aligned}
D^* &= \kappa_{AA}D_{AA} + \kappa_{Aa}D_{Aa} + \kappa_{aa}D_{aa}, & (4.23)\\
D^\dagger &= \xi_{AA}D_{AA} + \xi_{Aa}D_{Aa} + \xi_{aa}D_{aa}, & (4.24)\\
L^\dagger &= \chi_{AA}L_{AA} + \chi_{Aa}L_{Aa} + \chi_{aa}L_{aa}, & (4.25)
\end{aligned}
$$

and use these to express the density effects of pupa cannibalism by adults (4.23) and egg cannibalism by adults (4.24) and larva (4.25). Each genotype i has a survival and transition matrix,

$$
\mathbf{U}_i = \begin{pmatrix} 0 & 0 & 0 \\ (1-\mu_i) & 0 & 0 \\ 0 & e^{-D^*} & (1-\nu_i) \end{pmatrix}, \tag{4.26}
$$

where μ_i is larval mortality rate and ν_i is adult mortality rate. In addition, each genotype i has a fertility matrix,

$$
\mathbf{F}_i = \begin{pmatrix} 0 & 0 & \beta_i e^{-L^\dagger - D^\dagger} \\ 0 & 0 & 0 \\ 0 & 0 & 0 \end{pmatrix}, \tag{4.27}
$$

where β_i is the fecundity at low densities. This parameterization permits selection to operate on any of the life-history characteristics; i.e. stage-specific viability, fertility, and/or cannibalism rates.

Genotype×stage dynamics   As an example of genotype×stage dynamics, we use parameters estimated from a laboratory population of *Tribolium* by Dennis et al. (1995) (Table 1). We introduce a hypothetical allele with additive effects on fecundity (parameter β). The simulation was initialized with a population of AA individuals with low fecundity at the equilibrium stage distribution. After 50 iterations, one larval heterozygote is introduced into the population with a fecundity exactly in between the two homozygotes. The invading allele with larger birthrate gradually takes over the population and becomes fixed. As the genetic composition of the population changes (Fig 4.1C and 4.1D), the population structure changes (Fig 4.1A and 4.1B). Eventually, as the population approaches the aa
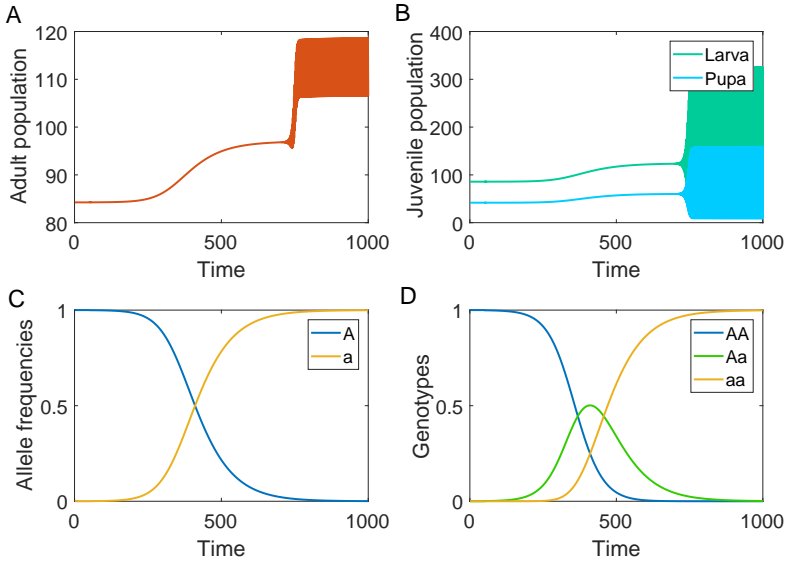
Figure 4.1: Eco-evolutionary dynamics of the invasion of an allele with a higher fecundity β ($\beta_{AA} = 5.68$, $\beta_{Aa} = 8.68$, $\beta_{aa} = 11.68$). All other parameters are taken from Table 1 in Dennis et al. (1995) and are set equal for all three genotypes: $\chi_i = 0.009264$, $\xi_i = 0.01097$, $\kappa_i = 0.01779$, $\mu_i = 0.5129$, $\nu_i = 0.1108$ for all i. **A**: abundance of the adult stage. **B**: abundance of larvae and pupae. **C**: frequencies of the A and a alleles. **D**: frequencies of the three genotypes.

boundary, the dynamics bifurcate from a stable equilibrium to a two-point cycle. Matlab code and parameters used for Figure 4.1 are in the Online Supplementary Materials.

4.4 The outcome of density-dependent selection: conditions for genotype coexistence

The most basic question about selection, density-dependent or otherwise, is the question of whether genotypes coexist, so that the population retains some degree of genetic diversity, or whether one allele becomes fixed. The question becomes more complicated, but no less basic, when demographic structure and nonlinearity are included. In this section, we present a general analytical criterion for determining the outcome of selection.

The dynamics of $\tilde{\mathbf{n}}$ take place in an ωg-dimensional space defined by combinations of ω stages and g genotypes (with $g = 3$ in the present context). In the absence of mutation, the ω-dimensional boundary subspaces defined by the
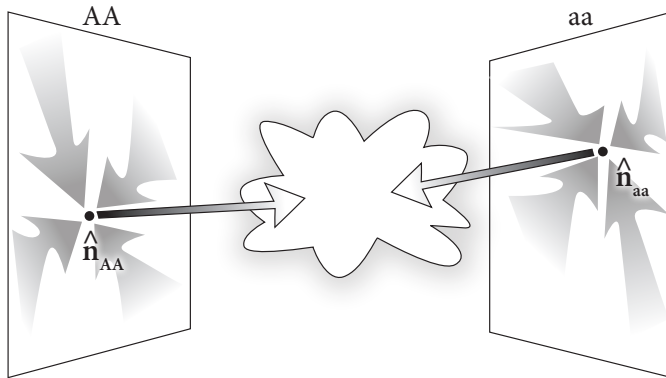
Figure 4.2: Graphical depiction of the ωg-dimensional space defined by combinations of ω stages and g genotypes. If both the homozygous boundaries are unstable, then a homozygote state can never be reached again once both alleles are present in the population (since both alleles grow when rare). Image by Jan van Arkel.

homozygous genotypes AA and aa are invariant under the dynamics specified by $\tilde{\mathbf{A}}\,[\tilde{\mathbf{n}}]$, and are given by the nonlinear projection matrices for the homozygous genotypes (Figure 4.2).

We assume the existence of a single equilibrium on each boundary, and that this equilibrium is stable with respect to perturbations in the boundary subspace.

Coexistence of the two alleles in a protected polymorphism (Levene 1953; Prout 1968; see Nagylaki 1992, Chap. 6) results when the boundary subspaces are both unstable to perturbations into the interior. That is, if allele A can invade a population of aa individuals and allele a can invade a population of AA individuals, then a homozygote state can never be reached again once both alleles are present in the population (since both alleles grow when rare). Mutual invasibility therefore leads to a protected genetic polymorphism.

In general, the dynamics in the interior are unknown, and could include multiple equilibria, strange attractors, cycles, etc. Provided both boundary subspaces are unstable to perturbations into the interior, we refer to any of the possible exotic dynamics in the interior as a protected polymorphism.

In general, nonlinear models could possess multiple invariant sets (equilibria, cycles, strange attractors) on the boundary. We will restrict our discussion to models with a unique equilibrium on the boundary. Extending the analysis to include a k-cycle on the boundary would be accomplished by transforming the

k-point cycle into an equilibrium of the k-point map, but we do not consider this here.

Stability of the homozygote boundaries

The stability of a boundary equilibrium is determined by the eigenvalue with the largest magnitude (i.e., the spectral radius) of the Jacobian matrix at the equilibrium. We denote this eigenvalue by ζ_{AA} and ζ_{aa} for the AA and aa boundaries, respectively. If $\zeta < 1$ the equilibrium is stable; otherwise it is unstable. We assume that the boundary equilibria are locally stable to perturbations within the boundary subspace, so if the equilibrium is unstable, the associated eigenvector must point into the interior, which implies that the invading allele increases when rare.

The Jacobian matrix,

$$\mathbf{M} = \left.\frac{\mathrm{d}\tilde{\mathbf{n}}(t+1)}{\mathrm{d}\tilde{\mathbf{n}}^{\mathsf{T}}(t)}\right|_{\hat{\mathbf{n}}}, \tag{4.28}$$

is obtained by differentiating equation (4.3) and evaluating the resulting derivative at the boundary equilibrium. We analyze the Jacobian at the AA boundary; the expression at the aa boundary can be derived afterwards by symmetry. The Jacobian matrix at the AA boundary is

$$\mathbf{M} = \tilde{\mathbf{A}}\left(\hat{\mathbf{n}}\right) + \underbrace{\left(\mathbf{e}_1 \otimes \hat{\mathbf{n}}_{AA}^{\mathsf{T}} \otimes \mathbf{I}_\omega\right)\left.\frac{\partial\mathrm{vec}\left(\mathbf{U}_{AA}\right)}{\partial\tilde{\mathbf{n}}^{\mathsf{T}}}\right|_{\hat{\mathbf{n}}} + \left(\mathbf{e}_1 \otimes \hat{\mathbf{n}}_{AA}^{\mathsf{T}} \otimes \mathbf{I}_\omega\right)\left.\frac{\partial\mathrm{vec}\left(\mathbf{F}_{AA}\right)}{\partial\tilde{\mathbf{n}}^{\mathsf{T}}}\right|_{\hat{\mathbf{n}}}}_{\text{Ecological nonlinearity}}$$

$$+ \underbrace{\left(\mathbf{e}_1 \otimes \mathbf{I}_\omega\right)\left(\mathbf{F}_{AA}\hat{\mathbf{n}}_{AA}\right)\left.\frac{\partial q_A}{\partial\tilde{\mathbf{n}}^{\mathsf{T}}}\right|_{\hat{\mathbf{n}}} - \left(\mathbf{e}_2 \otimes \mathbf{I}_\omega\right)\left(\mathbf{F}_{AA}\hat{\mathbf{n}}_{AA}\right)\left.\frac{\partial q_A}{\partial\tilde{\mathbf{n}}^{\mathsf{T}}}\right|_{\hat{\mathbf{n}}}}_{\text{Genetic nonlinearity}}, \tag{4.29}$$

see Appendix 4.A for a derivation. The linearization reflects the two sources of nonlinearity in the model: those due to ecological density dependence and those due to the genetic frequency-dependence.

The matrix $\mathbf{M}$ is a block structured matrix with blocks corresponding to genotypes and entries within the blocks corresponding to stages within genotypes,

$$\mathbf{M} = \left(\begin{array}{c|c|c} \mathbf{M}_{11} & \mathbf{M}_{12} & \mathbf{M}_{13} \\ \hline \mathbf{M}_{21} & \mathbf{M}_{22} & \mathbf{M}_{23} \\ \hline \mathbf{M}_{31} & \mathbf{M}_{32} & \mathbf{M}_{33} \end{array}\right), \tag{4.30}$$

where block $\mathbf{M}_{11}$ represents the contribution of perturbations in the AA direction to growth or decline of perturbations in the AA direction, block $\mathbf{M}_{12}$ represents

the contribution of perturbations in the Aa direction to growth or decline of perturbations in the AA direction, etc. All of the block terms in the Jacobian are given, with their derivation, in Appendix 4.A.

Evaluated at the equilibrium on the AA boundary, the Jacobian matrix $\mathbf{M}$ is block upper triangular, with

$$\mathbf{M}_{21} = \mathbf{M}_{31} = \mathbf{M}_{32} = \mathbf{0}, \tag{4.31}$$

(See equation (4.A35) in Appendix 4.A). Thus the spectral radius of $\mathbf{M}$ depends on the eigenvalues of the diagonal blocks. Block $\mathbf{M}_{33} = \mathbf{U}_{aa}$ projects perturbations in the aa direction, and since $\rho(\mathbf{U}_{aa}) < 1$ this direction is always stable. Block $\mathbf{M}_{11}$ projects perturbations within the AA boundary. By assumption, the boundary equilibrium is stable to such perturbations, so the spectral radius of $\mathbf{M}_{11}$ is less than one. The stability of the AA boundary equilibrium therefore depends on the eigenvalues of the submatrix $\mathbf{M}_{22}$,

$$\mathbf{M}_{22} \;=\; \left(\mathbf{U}_{Aa}\left(\hat{\mathbf{n}}\right) + \frac{1}{2}\mathbf{F}_{Aa}\left(\hat{\mathbf{n}}\right) + \frac{1}{2N_{\mathrm{b}}}(\mathbf{F}_{AA}\hat{\mathbf{n}}_{AA}) \otimes \mathbf{c}_{Aa}^{\mathsf{T}} \right), \tag{4.32}$$

where N_b is the number of individuals that are in a breeding stage at the equilibrium (see Appendix 4.A).

We denote the spectral radius of $\mathbf{M}_{22}$ as

$$\zeta_{AA} = \rho\left(\mathbf{M}_{22}\right) \tag{4.33}$$

where $\rho(\cdot)$ denotes the maximum eigenvalue of a matrix. By symmetry, the dominant eigenvalue of the Jacobian matrix at the aa boundary, denoted by ζ_{aa}, is obtained by replacing AA by aa in (4.32).

Criteria for a polymorphism A protected polymorphism occurs when both boundaries are unstable, i.e. when

$$\zeta_{AA} > 1 \quad \text{and} \quad \zeta_{aa} > 1. \tag{4.34}$$

Equation (4.34) is satisfied if and only if

$$\rho\left(\mathbf{U}_{Aa}\left(\hat{\mathbf{n}}\right) + \frac{1}{2}\mathbf{F}_{Aa}\left(\hat{\mathbf{n}}\right) + \frac{1}{2N_{\mathrm{b}}}(\mathbf{F}_{AA}\hat{\mathbf{n}}_{AA}) \otimes \mathbf{c}_{Aa}^{\mathsf{T}} \right) \;>\; 1, \tag{4.35}$$

$$\rho\left(\mathbf{U}_{Aa}\left(\hat{\mathbf{n}}\right) + \frac{1}{2}\mathbf{F}_{Aa}\left(\hat{\mathbf{n}}\right) + \frac{1}{2N_{\mathrm{b}}}(\mathbf{F}_{aa}\hat{\mathbf{n}}_{aa}) \otimes \mathbf{c}_{Aa}^{\mathsf{T}} \right) \;>\; 1. \tag{4.36}$$

We note that the conditions for polymorphism in equations (4.35) and (4.36) are a function of the nonlinear demographic rates of both the invading heterozygote and the resident homozygote (through the $\mathbf{U}_i$ and $\mathbf{F}_i$ matrices) and of the equilibrium structure of the homozygote equilibrium, $\hat{\mathbf{n}}_{AA}$ or $\hat{\mathbf{n}}_{aa}$.

4.5 *Tribolium* revisited: density-dependent selection and pesticide resistance

Armed with these coexistence conditions, we return to *Tribolium* to study the spread of malathion resistance in the red flour beetle, *Tribolium castaneum*. Malathion was a commonly used pesticide in grain storage in the 1950s, and malathion resistance has since become widespread in *Tribolium castaneum*. The evolution of pesticide resistance is usually assumed to involve a fitness trade-off, in which resistant genotypes are at a disadvantage in the absence of the pesticide. However, there appears to be no fitness trade-off related to malathion resistance in *T. castaneum*. The resistant strain appears to have higher fitness even in the absence of malathion (Haubruge and Arnaud 2001; Cheung 2002; Arnaud et al. 2005). Arnaud et al. (2005) suggest that the higher fitness of malathion resistant genes may be the result of posterior modification of the insect genome after resistance became prevalent.

The genetics of malathion resistance varies among strains; sometimes resistance is found to be polygenic, while in other strains, it is due to a dominant allele at a single autosomal locus (Wool et al. 1982). Cheung (2002) studied a *Tribolium* strain in which resistance is primarily controlled by a single, dominant allele or closely linked set of alleles. We denote the resistant allele with r and the susceptible allele with s, the genotypes are ss, rs, and rr. Since the resistant allele is almost completely dominant, Cheung assumed that the demographic rates of the rs genotype are identical to the demographic rates of the rr genotype, i.e.

$$\mathbf{U}_{rr}\left(\tilde{\mathbf{n}}\right) = \mathbf{U}_{rs}\left(\tilde{\mathbf{n}}\right), \tag{4.37}$$

$$\mathbf{F}_{rr}\left(\tilde{\mathbf{n}}\right) = \mathbf{F}_{rs}\left(\tilde{\mathbf{n}}\right), \tag{4.38}$$

for any population vector $\tilde{\mathbf{n}}$.

Cheung estimated $\mathbf{U}_{ss}$, $\mathbf{F}_{ss}$, $\mathbf{U}_{rr}$, and $\mathbf{U}_{rr}$ in the laboratory under three levels of malathion exposure (0 ppm, 1.5 ppm, and 3 ppm). Experimental populations were kept in 120 ml Wheaton vials containing 20 grams of media (92.5% bleached white flour, 5% dry brewer's yeast, 1.5% ground fumigation, and 1% sunflower oil). The media containing 1.5 ppm and 3 ppm malathion was prepared by diluting malathion into the sunflower oil before adding to the flour. Each malathion treatment was initiated with 250 larva, 5 pupa, and 250 adults.

Three treatment groups were established, with different initial allele frequencies and four replicate populations in each treatment group. Populations in the two homozygous boundary treatments were initiated with all ss and rr insects. In the "evolving treatment" each population was initiated with all ss larvae and pupae, and with 245 ss and 5 rs adults, resulting in an initial r allele frequency

Table 4.2: Parameter estimates for malathion resistant and susceptible strains at 3 ppm malathion, from Table 2 in Cheung (2002). Heterozygote parameters are assumed to be identical to the resistant homozygote.

| Parameter	rr	ss
β	9.650	0.6564
χ	0.006730	0.005727
ξ	0.009901	0.0
κ	0.01051	0.01330
μ	0.1115	0.6586
ν	0.5	0.5

of 0.01 among adults. All life stages in each population were counted once every two weeks for 80 weeks (t = 40). Adult mortality was set at 50% by removing half the number of adults counted in the previous census minus the number of dead adults found in the current census. One of the replicate populations in the evolving treatment group was lost to disease at week 56 (t = 28). Parameters for rr and ss genotypes were estimated from homozygous populations with a maximum likelihood procedure, which is described in section 2 of Cheung (2002). The parameter values are given in Table 4.2.

Dynamics under pesticide exposure
Figure 4.3 shows adult abundance data from Cheung's experiments at 3 ppm malathion and the results of projections from the *Tribolium* model using the parameters in Table 4.2. Under these conditions, a homozygous ss population goes extinct (Figure 4.3a), and a population of homozygous rr individuals persists at a stable equilibrium (Figure 4.3c). When a small number of heterozygote rs individuals are introduced into a susceptible population, evolutionary rescue saves the population from extinction (Figure 4.3b).[2] MATLAB code and parameters used for Figure 4.3 are in the Online Supplementary Materials.

Cheung (2002) estimated allele frequencies at the end of the experiment ($t = 40$) in the three surviving populations of the evolving treatment group by sampling and isolating 45-50 large larva or pupa, mating them with ss genotypes, and testing the survival of their offspring in malathion media to determine the genotypes of the sampled insects. This yielded estimates of the frequency of the r allele of 0.857, 0.948, and 0.889, with a mean and standard error of 0.898±0.027. In comparison, at $t = 40$, the model predicts a frequency of the r allele of 0.862, which is not statistically different from the mean experimental value ($p = 0.31$).

---

[2]Noise-induced oscillations occur in the resistant *Tribolium* populations because the attractor on the resistant boundary is near the bifurcation threshold to a stable period-two cycle.
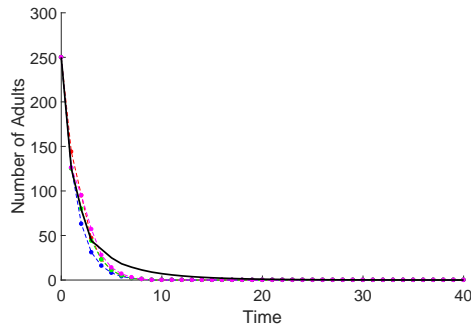
(a) Population of susceptible *Tribolium* individuals at 3 ppm malathion.
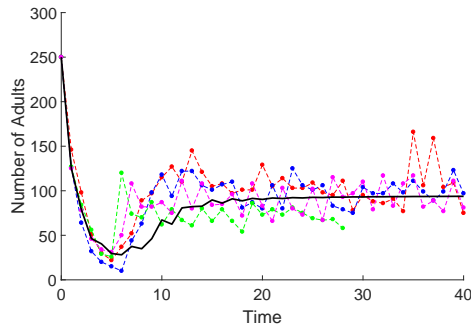
(b) An evolving *Tribolium* population of individuals at 3 ppm malathion, initial frequency of r allele is 0.01.
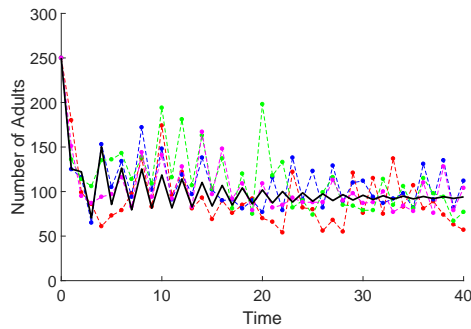
(c) Population of resistant *Tribolium* individuals at 3 ppm malathion.

Figure 4.3: Adult abundance summed over genotypes, solid black line is simulated, dashed lines are data from replicates. 4.3a. Population dynamics on the susceptible boundary at 3 ppm malathion. 4.3b. Population dynamics of an evolving *Tribolium* population. Initially the frequency of the r allele among adults is 0.01. 4.3c. Population dynamics on the resistant boundary at 3 ppm malathion.

Boundary stability

The stability of a population of the susceptible *Tribolium* to invasion by the resistant allele is determined by the dominant eigenvalue ζ_{ss} of the Jacobian. The final term in (4.35) simplifies significantly because the *Tribolium* model contains only one reproducing stage. If we denote the stage abundances at the susceptible equilibrium by $\hat{L}_{ss}$, $\hat{P}_{ss}$, $\hat{D}_{ss}$, then

$$\frac{1}{2N_{\mathrm{b}}} \left(\mathbf{F}_{ss}\left(\hat{\mathbf{n}}\right) \hat{\mathbf{n}}_{ss} \right) \otimes \mathbf{c}_{rs}^{\mathsf{T}} \;=\; \frac{\left(\beta_{ss} \hat{A}_{ss} e^{-\kappa_{el,ss}\hat{L}_{ss} - \kappa_{ea,ss}\hat{A}_{ss}} \right) \mathbf{e}_1 \otimes \mathbf{e}_3^{\mathsf{T}}}{\hat{A}_{ss}} \quad (4.39)$$

$$= \; \mathbf{F}_{ss}(\hat{\mathbf{n}}_{ss}). \quad (4.40)$$

Thus the *ss* equilibrium will be invaded by the resistant allele if

$$\zeta_{ss} \;=\; \rho \begin{pmatrix} 0 & 0 & \frac{1}{2}\left(\beta_{rs} + \beta_{ss}\right) e^{-\chi_{ss}\hat{L}_{ss} - \xi_{ss}\hat{D}_{ss}} \\ (1 - \mu_{rs}) & 0 & 0 \\ 0 & e^{-\kappa_{ss}\hat{D}_{ss}} & (1 - \nu_{rs}) \end{pmatrix} > 1 \quad (4.41)$$

At 3 ppm malathion, $\zeta_{ss} = 1.8450$, so the resistant allele is able to invade. In the absence of malathion, $\zeta_{ss} = 1.0265$, so the resistant allele is superior, even without the advantage of the presence of malathion.

Since the model assumes complete dominance, the rs and rr individuals have identical parameters. This implies that $\zeta_{rr} = 1$, and that linearization fails to show the stability of the equilibrium. This is a well known phenomenon in models for selection against recessive alleles (e.g., Nagylaki 1992, Sect. 4.2). Because recessive homozygotes are so rare close to the dominant equilibrium, elimination of the recessive is extremely slow. Simulations, however, show that the resistant boundary is stable to invasion by the susceptible allele.

Evolutionary stability analysis The analytical expression for stability of the homozygote boundaries allows us to study the effect of parameter changes on stability; i.e., we can perform an evolutionary stability analysis. To demonstrate such an analysis, we analyze the effects on stability of the degree of dominance of the resistant allele. This analysis was inspired by Beeman (1983) who found incomplete dominance of the resistant allele in the *Rmal* strain of *Tribolium* at high concentrations of malathion.

We analyze the effect of incomplete dominance by writing the heterozygote parameters as a convex combination of the parameters of the homozygotes; e.g., for mortality,

$$\mu_{rs} = (1 - x)\mu_{rr} + x\mu_{ss}, \quad (4.42)$$

and likewise for all other parameters in the model. The parameter x weighs the relative effect of the two alleles on all vital rates in heterozygotes. When $x = 1$, the s allele is dominant and when $x = 0$ the r allele is dominant.

Figure 4.4a shows the dominant eigenvalue ζ evaluated at both boundaries as a function of x. The ss boundary is unstable in the range $[0, 1)$; the rr boundary is stable in the range $(0, 1]$.

Figure 4.4b shows the effect of dominance on the fixation time, defined as the time required to reduce the frequency of the susceptible allele from 0.99 to 0.01 in the larvae. Alternative definitions of fixation time involving sums of stages rather than only the larval stage result in the same qualitative shape. Using a different threshold to define allele fixation does effect the shape of the curve. The initial increase of the resistant allele is faster at $x = 0$ than at $x = 0.5$, but the final approach to the boundary is faster at $x = 0.5$. If we had defined competitive exclusion as the susceptible allele having a frequency less than 0.2 in larvae, the line in Figure 4.4b would be monotonically increasing with x.

4.6 Discussion

Demographic models classify individuals into i-states, such as age classes or developmental stages. The i-state captures all the relevant information about an individual such that the fate of an individual depends only on its current i-state and the environment (Metz 1977; Caswell and John 1992; Caswell 2001). In this paper, we extended the i-state to include individual genotype. By treating genotype as a demographic state variable, the powerful mathematical machinery of matrix population models becomes available to study genotype×stage dynamics (Figures 4.1 and 4.3), and the powerful mathematical machinery of matrix calculus becomes available to perform stability analysis via linearization (Sections 4.4 and 4.5). Using such a linearization, we obtained conditions for the coexistence of two alleles at one locus for a general density-dependent demographic model with age- or stage-structure. This opens new possibilities for eco-evolutionary analysis of life history traits. It complements, but is not intended to replace, the quantitative genetics approaches recently developed by Coulson et al. (2010).

We applied the model to study the genotype×stage dynamics of pesticide resistance in *Tribolium castaneum*. The model does an excellent job of describing experimental populations exposed to malathion, and successfully predicts the outcome of selection (fixation of the resistant allele). Fixation would occur more quickly for intermediate dominance than than for complete dominance (Figure 4.4b).
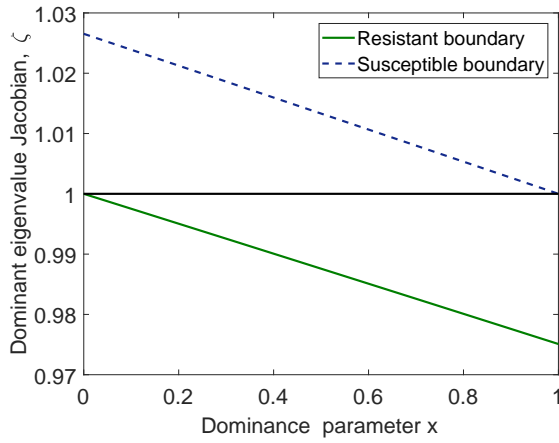
(a) The effect of incomplete dominance on boundary stability as measured by the dominant eigenvalue of the Jacobian. At $x = 0$ the resistant allele is completely dominant, and at $x = 1$ the susceptible allele is completely dominant.
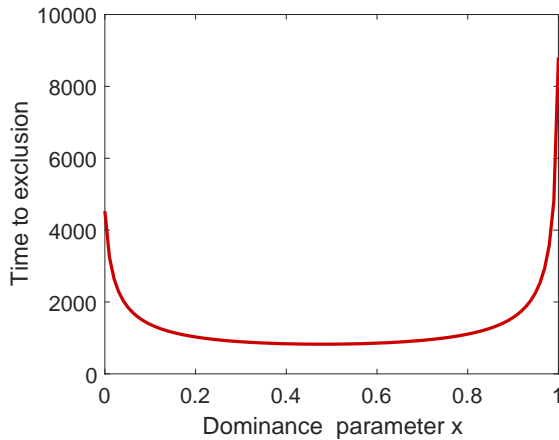
(b) The effect of incomplete dominance on the time to allele fixation. At $x = 0$ the resistant allele is dominant; at $x = 1$ the susceptible allele is dominant.

The invasion speed of a pesticide-resistant allele in an agricultural pest is an important quantity for agriculturalists and/or policy makers. Pesticide resistance in insects is often determined by only one or two loci (Roush and McKenzie 1987; Ffrench-Constant et al. 2004). For example, a number of single gene mutations are known to result in DDT resistance in *Drosophila* (Pittendrigh et al. 1997; Joußen et al. 2008). Similarly, a single gene was found in houseflies that influences the rate of penetration of DDT and dieldrin by Hoyer and Plapp Jr (1968). There are many more examples, see reviews by Georghiou (1969), Roush and McKenzie (1987), or Ffrench-Constant et al. (2004). The one locus, two allele model presented in this paper could therefore be applicable to many cases of insecticide resistance.

Maximization principles Early work on density-dependent selection focused on the maximization of equilibrium population size (hence "K-selection"; MacArthur (1962); MacArthur and Wilson (1967); Roughgarden (1971)). Charlesworth (1994) extended this result to age-structured populations and showed that density-dependent selection maximizes the abundance of the age class that is exerting the density-dependent pressure on the population. For example, if adults are cannibalizing juveniles and juvenile mortality is a nonlinear function of adult density, then a successful invasion will always lead to a higher adult density. In deriving this result, Charlesworth assumes males and females have identical demographic rates, i.e. there is no sexual dimorphism in any life-history characteristics.

Because one cannot, in general, find expressions for equilibria in nonlinear matrix population models, we do not consider maximization of density here. Moreover, we note that in a structured model there is no reason to assume that "density" is a single scalar quantity (e.g., Caswell et al. 2004). Each stage may have its own effects on other stages; a total density obtained by adding together tiny seedlings and big trees has little biological meaning. Equally, each vital rate may be influenced by a different set of stages, as in the *Tribolium* model where fertility is a function of larval and adult densities, but pupal survival depends only on adult density. Thus maximization of "density" will not be as simple a concept in structured models as it is in unstructured models.

Extensions The model presented here can be extended by relaxing a number of assumptions. Our assumption of female dominance leads to the assumption that male and female population vectors are proportional, so that the female population vector can be used to calculate gene frequencies in the (male) mating population. de Vries and Caswell (2018b) show that this assumption is met provided males

and females have equal survival and transition probabilities, and are born at equal proportions. Both these assumptions could be relaxed in a two-sex model.

The model could also be extended to include more ecological interaction, such as time-dependent demographic rates, interactions among species, or dependence on environmental resources. The genetic component of the model can be expanded to include nonrandom mating, more than two alleles, or mutations.

At the cost of additional mathematics, our results could be extended to dynamics on the boundaries that are more exotic than fixed points. A k-point cycle, for example, can be transformed into an equilibrium by studying the k-point map, i.e. by applying the projection matrix k times.

We did not discuss frequency-dependent selection in this paper, in which the vital rates of an individual would be a function of the frequencies of the other genotypes in the population. Negative frequency-dependent selection, in which the fitness of each genotype declines as its frequency increases, is often invoked as a mechanisms for maintaining polymorphisms. In a structured population, the demographic rates could depend on the genotype frequencies in some subset of stages rather than in the entire population. In species with alternative mating strategies, the mating strategies often show negative frequency dependence (e.g., studies of salmon by Gross 1985; Berejikian et al. 2010). Incorporating frequency dependence in our model would permit analysis of such traits.

The model construction introduced in this paper remains unchanged for frequency-dependent models, or for models with both frequency-dependence and density dependence. However, a model with only frequency-dependence becomes linear on the boundaries. Therefore the population is either exponentially growing or shrinking rather than at equilibrium on the boundary. To calculate the stability of the homozygote population to invasion by the other allele in a frequency-dependent model, it is necessary to renormalize the population vector and to project the resulting frequency vector instead, as is discussed in de Vries and Caswell (2018a).

Conclusion   We began this paper by emphasizing how demographic and genetic processes combine to determine eco-evolutionary dynamics. At this point we have shown several examples of how Mendelian genetics and density-dependent vital rates, combined into a stage×genotype-structured matrix model, can be used to this end. The genotypes determine survival, transitions, and fertility. The rules of mating and segregation determine the genetic composition of offspring. The model can project dynamics of joint stage×genotype distributions, for hypothetical (Figure 4.1) and experimental (Figure 4.3) situations. The eventual genetic

coexistence is determined by stability analysis of the homozygous boundary equilibria.

Acknowledgments

Appendix 4.A   Derivation of Jacobian matrix, general nonlinear model

The stability of a homozygote boundary equilibrium is determined by the largest absolute eigenvalue (spectral radius) of the Jacobian matrix of the nonlinear matrix model evaluated at the boundary equilibrium. We denote the spectral radius of the Jacobian at the AA boundary by ζ_{AA}, and at the aa boundary by ζ_{aa}. If the magnitude of the dominant eigenvalue of the Jacobian matrix is larger than one when evaluated at an equilibrium, then this equilibrium is unstable. The Jacobian matrix,

$$\mathbf{M} = \frac{d\tilde{\mathbf{n}}(t+1)}{d\tilde{\mathbf{n}}^{\mathsf{T}}(t)}\bigg|_{\hat{\mathbf{n}}}, \tag{4.A1}$$

is obtained by differentiating equation (4.3),

$$\tilde{\mathbf{n}}(t+1) = \tilde{\mathbf{A}}\left[\tilde{\mathbf{n}}\right]\tilde{\mathbf{n}}(t), \tag{4.A2}$$

and evaluating the resulting derivative at the boundary equilibrium. This requires a long series of matrix calculus operations (Magnus and Neudecker 1985; Caswell 2008). The analysis repeatedly takes advantage of the fact that $\hat{\mathbf{n}}$ at the AA boundary contains zeros for the blocks corresponding to Aa and aa genotypes.

Differentiate equation (4.A2) to obtain

$$d\tilde{\mathbf{n}}(t+1) = \tilde{\mathbf{A}}d\tilde{\mathbf{n}}(t) + \left(d\tilde{\mathbf{A}}\right)\tilde{\mathbf{n}}(t), \tag{4.A3}$$

where the explicit dependence of $\tilde{\mathbf{A}}$ on $\tilde{\mathbf{n}}$ has been omitted to avoid a cluttering of brackets. Multiply the second term by an $\omega g \times \omega g$ identity matrix,

$$d\tilde{\mathbf{n}}(t+1) = \tilde{\mathbf{A}}d\tilde{\mathbf{n}}(t) + \mathbf{I}_{\omega g}\left(d\tilde{\mathbf{A}}\right)\tilde{\mathbf{n}}(t). \tag{4.A4}$$

and apply the vec operator to both sides, remembering that as $\tilde{\mathbf{n}}$ is a vector, $\text{vec}\tilde{\mathbf{n}} = \tilde{\mathbf{n}}$,

$$d\tilde{\mathbf{n}}(t+1) = \tilde{\mathbf{A}}d\tilde{\mathbf{n}}(t) + \text{vec}\left[\mathbf{I}_{\omega g}\left(d\tilde{\mathbf{A}}\right)\tilde{\mathbf{n}}(t)\right]. \tag{4.A5}$$

Next apply Roth's theorem (Roth 1934), $\text{vec}\mathbf{ABC} = (\mathbf{C}^{\mathsf{T}} \otimes \mathbf{A})\text{vec}\mathbf{B}$, to replace the vec operator with the Kronecker product:

$$d\tilde{\mathbf{n}}(t+1) = \tilde{\mathbf{A}}d\tilde{\mathbf{n}}(t) + \left(\tilde{\mathbf{n}}^{\mathsf{T}}(t) \otimes \mathbf{I}_{\omega g}\right)d\text{vec}\left[\tilde{\mathbf{A}}\right]. \tag{4.A6}$$

The matrix $\tilde{\mathbf{A}}$ can be decomposed into nine $\omega \times \omega$ block matrices, which are created by adding equations 4.22 and 4.20:

$$\tilde{\mathbf{A}}(\tilde{\mathbf{n}}) = \left(\begin{array}{c|c|c} \mathbf{U}_{AA} + q_A^{\text{b}}\mathbf{F}_{AA} & \frac{1}{2}q_A^{\text{b}}\mathbf{F}_{Aa} & \mathbf{0} \\ \hline q_a^{\text{b}}\mathbf{F}_{AA} & \mathbf{U}_{Aa} + \frac{1}{2}\mathbf{F}_{Aa} & q_A^{\text{b}}\mathbf{F}_{aa} \\ \hline \mathbf{0} & \frac{1}{2}q_a^{\text{b}}\mathbf{F}_{Aa} & \mathbf{U}_{aa} + q_a^{\text{b}}\mathbf{F}_{aa} \end{array}\right). \tag{4.A7}$$

The blocks are denoted by $\mathbf{A}_{ij}$, so that for example

$$\mathbf{A}_{11} = \mathbf{U}_{AA} + q_A \mathbf{F}_{AA}, \tag{4.A8}$$

and

$$\mathbf{A}_{31} = \mathbf{0}. \tag{4.A9}$$

The matrix $\tilde{\mathbf{A}}$ can then be written as

$$\tilde{\mathbf{A}} \;=\; \sum_{i,j=1}^{3} \mathbf{E}_{ij} \otimes \mathbf{A}_{ij}, \tag{4.A10}$$

$$=\; \sum_{i,j=1}^{3} \left(\mathbf{e}_i \mathbf{e}_j^{\mathsf{T}}\right) \otimes \left(\mathbf{A}_{ij}\mathbf{I}_\omega\right), \tag{4.A11}$$

where we have used the definition of the matrix $\mathbf{E}_{ij} = \mathbf{e}_i \mathbf{e}_j^{\mathsf{T}}$. Using $\mathbf{AC} \otimes \mathbf{BD} = (\mathbf{A} \otimes \mathbf{B})(\mathbf{C} \otimes \mathbf{D})$, equation (4.A11) can be rewritten as

$$\tilde{\mathbf{A}} = \sum_{i,j=1}^{3} \left(\mathbf{e}_i \otimes \mathbf{A}_{ij}\right) \left(\mathbf{e}_j^{\mathsf{T}} \otimes \mathbf{I}_\omega\right). \tag{4.A12}$$

Next use the identity $\sum_i \left(\mathbf{e}_i \otimes \mathbf{I}_\omega\right) \mathbf{A}_{ij} = \sum_i \mathbf{e}_i \otimes \mathbf{A}_{ij}$ to write

$$\tilde{\mathbf{A}} = \sum_{i,j=1}^{3} \left(\mathbf{e}_i \otimes \mathbf{I}_\omega\right) \mathbf{A}_{ij} \left(\mathbf{e}_j^{\mathsf{T}} \otimes \mathbf{I}_\omega\right). \tag{4.A13}$$

This yields the following formula for $\mathrm{vec}\mathbf{A}$:

$$\mathrm{vec}\tilde{\mathbf{A}} = \sum_{i,j}^{3} \left(\mathbf{e}_j \otimes \mathbf{I}_\omega\right) \otimes \left(\mathbf{e}_i \otimes \mathbf{I}_\omega\right) \mathrm{vec}\mathbf{A}_{ij}. \tag{4.A14}$$

Armed with this expression for $\mathrm{vec}\tilde{\mathbf{A}}$, we analyze the term $\left(\tilde{\mathbf{n}}^{\mathsf{T}}(t) \otimes \mathbf{I}_{\omega g}\right) \mathrm{dvec}\tilde{\mathbf{A}}$ in (4.A6). Replace the derivative of $\mathrm{vec}\tilde{\mathbf{A}}$ with equation (4.A14), such that

$$\left(\tilde{\mathbf{n}}^{\mathsf{T}}(t) \otimes \mathbf{I}_{\omega g}\right) \mathrm{dvec}\tilde{\mathbf{A}} = \sum_{i,j=1}^{3} \left(\tilde{\mathbf{n}}^{\mathsf{T}}(t) \otimes \mathbf{I}_{\omega g}\right) \left[\left(\mathbf{e}_j \otimes \mathbf{I}_\omega\right) \otimes \left(\mathbf{e}_i \otimes \mathbf{I}_\omega\right)\right] \mathrm{dvec}\mathbf{A}_{ij}$$

$$\tag{4.A15}$$

Use $\left(\mathbf{A} \otimes \mathbf{B}\right)\left(\mathbf{C} \otimes \mathbf{D}\right) = \mathbf{AC} \otimes \mathbf{BD}$ to rewrite

$$\left(\tilde{\mathbf{n}}^{\mathsf{T}}(t) \otimes \mathbf{I}_{\omega g}\right) \left[\left(\mathbf{e}_j \otimes \mathbf{I}_\omega\right) \otimes \left(\mathbf{e}_i \otimes \mathbf{I}_\omega\right)\right] = \left(\tilde{\mathbf{n}}^{\mathsf{T}} \left(\mathbf{e}_j \otimes \mathbf{I}_\omega\right)\right) \otimes \left(\mathbf{I}_{\omega g}\left(\mathbf{e}_i \otimes \mathbf{I}_\omega\right)\right), \tag{4.A16}$$

substituting this expression into the right hand side of equation (4.A15) yields

$$\left(\tilde{\mathbf{n}}^{\mathsf{T}}(t) \otimes \mathbf{I}_{\omega g}\right) \mathrm{dvec}\tilde{\mathbf{A}} = \sum_{i,j=1}^{3} \left(\tilde{\mathbf{n}}^{\mathsf{T}} \left(\mathbf{e}_j \otimes \mathbf{I}_\omega\right)\right) \otimes \left(\mathbf{e}_i \otimes \mathbf{I}_\omega\right) \mathrm{dvec}\mathbf{A}_{ij}. \tag{4.A17}$$

When we evaluate this expression on the boundary, only AA individuals are present, i.e.

$$\hat{\mathbf{n}}^{\mathsf{T}}(t) = \left(\hat{\mathbf{n}}_{AA}^{\mathsf{T}}, \mathbf{0}, \mathbf{0}\right). \tag{4.A18}$$

Substituting this expression for $\tilde{\mathbf{n}}^{\mathsf{T}}(t)$ into equation (4.A17), so that only terms with $j = 1$ are nonzero, yields

$$\left[\left(\tilde{\mathbf{n}}^{\mathsf{T}}(t) \otimes \mathbf{I}_{\omega g}\right) \mathrm{dvec}\tilde{\mathbf{A}}\right]\bigg|_{\hat{\mathbf{n}}} = \sum_{i}^{3} \hat{\mathbf{n}}_{AA}^{\mathsf{T}} \otimes \left(\mathbf{e}_i \otimes \mathbf{I}_{\omega}\right) \mathrm{dvec}\mathbf{A}_{i1}\bigg|_{\hat{\mathbf{n}}}. \tag{4.A19}$$

The $\mathbf{A}_{i1}$ matrices are the matrices in the first block column of $\tilde{\mathbf{A}}$, see equation (4.A7), i.e.

$$\mathbf{A}_{11} = \mathbf{U}_{AA}\left(\tilde{\mathbf{n}}\right) + q_A^{\mathrm{b}}\mathbf{F}_{AA}\left(\tilde{\mathbf{n}}\right), \tag{4.A20}$$
$$\mathbf{A}_{21} = (1 - q_A^{\mathrm{b}})\mathbf{F}_{AA}\left(\tilde{\mathbf{n}}\right), \tag{4.A21}$$
$$\mathbf{A}_{31} = \mathbf{0}, \tag{4.A22}$$

where we have used that $q_a^{\mathrm{b}} = 1 - q_A^{\mathrm{b}}$. Finally, using these expressions for the $\mathbf{A}_{i1}$ matrices and equation (4.A19) to evaluate equation (4.A6) on the AA boundary yields

$$\begin{aligned}
\mathrm{d}\tilde{\mathbf{n}}(t+1) &= \tilde{\mathbf{A}}\mathrm{d}\tilde{\mathbf{n}}(t) + \left(\hat{\mathbf{n}}_{AA}^{\mathsf{T}} \otimes \mathbf{e}_1 \otimes \mathbf{I}_{\omega}\right) \mathrm{dvec}\left[\mathbf{U}_{AA}\left(\tilde{\mathbf{n}}\right)\right] \\
&+ \left(\hat{\mathbf{n}}_{AA}^{\mathsf{T}} \otimes \mathbf{e}_1 \otimes \mathbf{I}_{\omega}\right) \mathrm{dvec}\left[q_A^{\mathrm{b}}\mathbf{F}_{AA}\left(\tilde{\mathbf{n}}\right)\right] \\
&+ \left(\hat{\mathbf{n}}_{AA}^{\mathsf{T}} \otimes \mathbf{e}_2 \otimes \mathbf{I}_{\omega}\right) \mathrm{dvec}\left[(1 - q_A^{\mathrm{b}})\mathbf{F}_{AA}\left(\tilde{\mathbf{n}}\right)\right],
\end{aligned} \tag{4.A23}$$

where the differentials on both sides are evaluated at the boundary equilibrium. Finally, using the first identification theorem and the chain rule together give the following formula for the Jacobian (Magnus and Neudecker 1985; Caswell 2008),

$$\begin{aligned}
\mathbf{M} &= \left.\frac{\mathrm{d}\tilde{\mathbf{n}}(t+1)}{\mathrm{d}\tilde{\mathbf{n}}(t)}\right|_{\hat{\mathbf{n}}}, \tag{4.A24} \\
&= \tilde{\mathbf{A}}\left(\hat{\mathbf{n}}\right) + \left(\hat{\mathbf{n}}_{AA}^{\mathsf{T}} \otimes \mathbf{e}_1 \otimes \mathbf{I}_{\omega}\right) \left.\frac{\partial \mathrm{vec}\left(\mathbf{U}_{AA}\right)}{\partial \tilde{\mathbf{n}}^{\mathsf{T}}}\right|_{\hat{\mathbf{n}}} \\
&+ \left(\hat{\mathbf{n}}_{AA}^{\mathsf{T}} \otimes \mathbf{e}_1 \otimes \mathbf{I}_{\omega}\right) \mathrm{vec}\left(\mathbf{F}_{AA}\right) \left.\frac{\partial q_A^{\mathrm{b}}}{\partial \tilde{\mathbf{n}}^{\mathsf{T}}}\right|_{\hat{\mathbf{n}}} + \left(\hat{\mathbf{n}}_{AA}^{\mathsf{T}} \otimes \mathbf{e}_1 \otimes \mathbf{I}_{\omega}\right) \left.\frac{\partial \mathrm{vec}\left(\mathbf{F}_{AA}\right)}{\partial \tilde{\mathbf{n}}^{\mathsf{T}}}\right|_{\hat{\mathbf{n}}} \\
&- \left(\hat{\mathbf{n}}_{AA}^{\mathsf{T}} \otimes \mathbf{e}_2 \otimes \mathbf{I}_{\omega}\right) \mathrm{vec}\left(\mathbf{F}_{AA}\right) \left.\frac{\partial q_A^{\mathrm{b}}}{\partial \tilde{\mathbf{n}}^{\mathsf{T}}}\right|_{\hat{\mathbf{n}}} \tag{4.A25}
\end{aligned}$$

Use that $\mathbf{a}\mathbf{b}^{\mathsf{T}} = \mathbf{a} \otimes \mathbf{b}^{\mathsf{T}} = \mathbf{b}^{\mathsf{T}} \otimes \mathbf{a}$ for two vectors $\mathbf{a}$ and $\mathbf{b}$ to write $\left(\hat{\mathbf{n}}_{AA}^{\mathsf{T}} \otimes \mathbf{e}_1 \otimes \mathbf{I}_{\omega}\right)$ as $\left(\mathbf{e}_1 \otimes \hat{\mathbf{n}}_{AA}^{\mathsf{T}} \otimes \mathbf{I}_{\omega}\right)$, and likewise for the term $\left(\hat{\mathbf{n}}_{AA}^{\mathsf{T}} \otimes \mathbf{e}_2 \otimes \mathbf{I}_{\omega}\right)$. Also note that the two terms with partial derivates of q_A can be rewritten using $\left(\mathbf{Z}^T \otimes \mathbf{X}\right)\mathrm{vec}\mathbf{Y} =$

vec $(\mathbf{XYZ})$ to obtain the following expression

$$
\begin{aligned}
\mathbf{M} \;=\;& \tilde{\mathbf{A}}\left(\hat{\mathbf{n}}\right) + \left(\mathbf{e}_1 \otimes \hat{\mathbf{n}}_{AA}^{\mathsf{T}} \otimes \mathbf{I}_\omega\right) \left.\frac{\partial \text{vec}\left(\mathbf{U}_{AA}\right)}{\partial \tilde{\mathbf{n}}^{\mathsf{T}}}\right|_{\hat{\mathbf{n}}} + \left(\mathbf{e}_1 \otimes \hat{\mathbf{n}}_{AA}^{\mathsf{T}} \otimes \mathbf{I}_\omega\right) \left.\frac{\partial \text{vec}\left(\mathbf{F}_{AA}\right)}{\partial \tilde{\mathbf{n}}^{\mathsf{T}}}\right|_{\hat{\mathbf{n}}} \\
&+\; \left(\mathbf{e}_1 \otimes \mathbf{I}_\omega\right)\left(\mathbf{F}_{AA}\hat{\mathbf{n}}_{AA}\right) \left.\frac{\partial q_A}{\partial \tilde{\mathbf{n}}^{\mathsf{T}}}\right|_{\hat{\mathbf{n}}} - \left(\mathbf{e}_2 \otimes \mathbf{I}_\omega\right)\left(\mathbf{F}_{AA}\hat{\mathbf{n}}_{AA}\right) \left.\frac{\partial q_A}{\partial \tilde{\mathbf{n}}^{\mathsf{T}}}\right|_{\hat{\mathbf{n}}} \quad (4.A26)
\end{aligned}
$$

To proceed, we need an expression for the partial derivative of the frequency of allele A in the breeding pool,

$$
\frac{\partial q_A^{\mathrm{b}}}{\partial \tilde{\mathbf{n}}^{\mathsf{T}}}. \tag{4.A27}
$$

Differentiating equation (4.12) from the main text,

$$
q_A^{\mathrm{b}} = \mathbf{e}_1^{\mathsf{T}}\mathbf{q}_b = \mathbf{e}_1^{\mathsf{T}}\mathbf{W}\mathbf{p}_b, \tag{4.A28}
$$

yields

$$
\frac{\partial q_A^{\mathrm{b}}}{\partial \tilde{\mathbf{n}}^{\mathsf{T}}} = \mathbf{e}_1^{\mathsf{T}}\mathbf{W}\frac{\partial \mathbf{p}_b}{\partial \tilde{\mathbf{n}}^{\mathsf{T}}}. \tag{4.A29}
$$

Combine equations (4.6) and (4.8) from the main text to write

$$
\mathbf{p}_b = \frac{\sum_{i=1}^g \left(\mathbf{E}_{ii} \otimes \mathbf{c}_i^{\mathsf{T}}\right) \tilde{\mathbf{n}}}{\sum_{j=1}^g \left(\mathbf{e}_j^{\mathsf{T}} \otimes \mathbf{c}_j^{\mathsf{T}}\right) \tilde{\mathbf{n}}}. \tag{4.A30}
$$

The denominator is the number of individuals in the population that are in a breeding stage, N_b. Taking the derivative of $\mathbf{p}_b$ yields

$$
\left.\frac{\partial \mathbf{p}_b}{\partial \tilde{\mathbf{n}}^{\mathsf{T}}}\right|_{\hat{\mathbf{n}}} = \frac{N_b \sum_{i=1}^3 \left(\mathbf{E}_{ii} \otimes \mathbf{c}_i^{\mathsf{T}}\right) - \sum_{i=1}^3 \left(\mathbf{E}_{ii} \otimes \mathbf{c}_i^{\mathsf{T}}\right) \hat{\mathbf{n}} \sum_{j=1}^3 \left(\mathbf{e}_j^{\mathsf{T}} \otimes \mathbf{c}_j^{\mathsf{T}}\right)}{\mathrm{N}_b^2}. \tag{4.A31}
$$

Writing above expression as a matrix yields

$$
\left.\frac{\partial \mathbf{p}_b}{\partial \tilde{\mathbf{n}}^{\mathsf{T}}}\right|_{\hat{\mathbf{n}}} = \frac{1}{N_b} \begin{pmatrix} 0 & -\mathbf{c}_{Aa}^{\mathsf{T}} & -\mathbf{c}_{aa}^{\mathsf{T}} \\ \mathbf{0}_\omega^{\mathsf{T}} & \mathbf{c}_{Aa}^{\mathsf{T}} & \mathbf{0}_\omega^{\mathsf{T}} \\ \mathbf{0}_\omega^{\mathsf{T}} & \mathbf{0}_\omega^{\mathsf{T}} & \mathbf{c}_{aa}^{\mathsf{T}} \end{pmatrix}. \tag{4.A32}
$$

Substituting equation (4.A32) into equation (4.A29) leads to

$$
\left.\frac{\partial q_A^{\mathrm{b}}}{\partial \tilde{\mathbf{n}}^{\mathsf{T}}}\right|_{\hat{\mathbf{n}}} = \mathbf{e}_1^{\mathsf{T}}\mathbf{W}\left.\frac{\partial \mathbf{p}_b}{\partial \tilde{\mathbf{n}}^{\mathsf{T}}}\right|_{\hat{\mathbf{n}}} \tag{4.A33}
$$

$$
= \begin{pmatrix} \mathbf{0} & -\frac{1}{2}\frac{\mathbf{c}_{Aa}^{\mathsf{T}}}{N_b} & -\frac{\mathbf{c}_{aa}^{\mathsf{T}}}{N_b} \end{pmatrix}. \tag{4.A34}
$$

Finally, plug equation (4.A34) back into the expression for the Jacobian, equation (4.A26), to write the Jacobian in terms of its block components,

$$
\mathbf{M} = \left(\begin{array}{c|c|c}
\mathbf{U}_{AA}(\hat{\mathbf{n}}) + \mathbf{F}_{AA}(\hat{\mathbf{n}}) & \frac{1}{2}\mathbf{F}_{Aa}(\hat{\mathbf{n}}) & \mathbf{0} \\
\hline
\mathbf{0} & \mathbf{U}_{Aa}(\hat{\mathbf{n}}) + \frac{1}{2}\mathbf{F}_{Aa}(\hat{\mathbf{n}}) & \mathbf{F}_{aa}(\hat{\mathbf{n}}) \\
\hline
\mathbf{0} & \mathbf{0} & \mathbf{U}_{aa}(\hat{\mathbf{n}})
\end{array} \right)
$$

$$
+ \left(\begin{array}{c|c|c}
\left(\hat{\mathbf{n}}_{AA}^{\mathsf{T}} \otimes \mathbf{I}_{\omega}\right) \frac{\partial \mathrm{vec}(\mathbf{U}_{AA}+\mathbf{F}_{AA})}{\partial \mathbf{n}_{AA}^{\mathsf{T}}} & \left(\hat{\mathbf{n}}_{AA}^{\mathsf{T}} \otimes \mathbf{I}_{\omega}\right) \frac{\partial \mathrm{vec}(\mathbf{U}_{AA}+\mathbf{F}_{AA})}{\partial \mathbf{n}_{Aa}^{\mathsf{T}}} & \left(\hat{\mathbf{n}}_{AA}^{\mathsf{T}} \otimes \mathbf{I}_{\omega}\right) \frac{\partial \mathrm{vec}(\mathbf{U}_{AA}+\mathbf{F}_{AA})}{\partial \mathbf{n}_{aa}^{\mathsf{T}}} \\
\hline
\mathbf{0} & \mathbf{0} & \mathbf{0} \\
\hline
\mathbf{0} & \mathbf{0} & \mathbf{0}
\end{array} \right)
$$

$$
+ \left(\begin{array}{c|c|c}
\mathbf{0} & -\frac{1}{2N_{\mathrm{b}}}(\mathbf{F}_{AA}\hat{\mathbf{n}}_{AA}) \otimes \mathbf{c}_{Aa}^{\mathsf{T}} & -\frac{1}{N_{\mathrm{b}}}(\mathbf{F}_{AA}\hat{\mathbf{n}}_{AA}) \otimes \mathbf{c}_{aa}^{\mathsf{T}} \\
\hline
\mathbf{0} & \frac{1}{2N_{\mathrm{b}}}(\mathbf{F}_{AA}\hat{\mathbf{n}}_{AA}) \otimes \mathbf{c}_{Aa}^{\mathsf{T}} & \frac{1}{N_{\mathrm{b}}}(\mathbf{F}_{AA}\hat{\mathbf{n}}_{AA}) \otimes \mathbf{c}_{aa}^{\mathsf{T}} \\
\hline
\mathbf{0} & \mathbf{0} & \mathbf{0}
\end{array} \right) . \tag{4.A35}
$$

This is the block-structured Jacobian matrix that appears in equation (4.30).